The compensator performance is shown in Fig. 2. A constant 2 kHz signal, corresponding to $\approx 10^{-3}$ rad RMS, was applied to the signal arm of the interferometer. Without compensation, the interferometer randomly drifts out of quadrature, as shown by trace *a*. The compensated output over an equal time interval is shown by trace *b*. This Figure shows that the signal sensitivity of the compensated output deviates by a peak of $\pm$ 1·6% over a 10 min interval, whereas the uncompensated output, derived from only one diode signal,

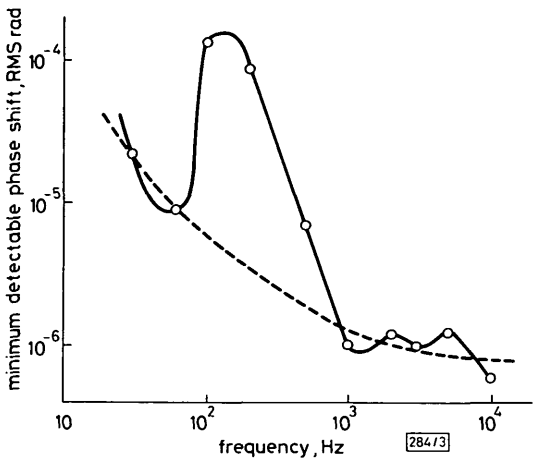

Fig. 3 *Minimum detectable phase shift as a function of frequency with compensated interferometer operating in laboratory environment*

Dashed line: see text

suffers complete fading several times. The minimum phase shift sensitivity (S/N $\approx$ 1) achieved with this interferometer working unshielded in a normal laboratory environment is shown in Fig. 3. The transfer function showed a flat frequency response from 28 Hz (3 dB point of the highpass filters) to 10 kHz with a linear dynamic range of > 120 dB.

The apparent decrease in the minimum phase sensitivity in a band between 100–500 Hz is attributed to environmental acoustical noise. Spectral analysis using sensitive microphonic detection confirmed the presence of a broadband source between 100–700 Hz. This noise peak was also present when the interferometer was actively compensated using a scheme similar to that previously described,[5] and consequently is not attributable to any fundamental cause. The dashed curve in Fig. 3 is an estimate of the minimum phase sensitivity in the absence of this noise source.

In conclusion, we have proposed, and demonstrated, the viability of a passive compensation scheme to maintain the sensitivity of a Mach-Zehnder interferometer at a maximum, thus eliminating the fading problem or the need for active compensation associated with homodyne detection. Passive compensation offers several advantages over active schemes, such as:

(i) elimination of noise associated with nonlinear feedback effects
(ii) infinite dynamic range of drift compensation
(iii) zero insertion loss.

The work was funded partly by the SERC and The Royal Society.

A. D. KERSEY
D. A. JACKSON
M. CORKE

Physics Laboratory
University of Kent at Canterbury
Canterbury, Kent CT2 7NR, England

5th March 1982

References

1 JACKSON, D. A., DANDRIDGE, A., and SHEEM, S. K.: 'Measurement of small phase shifts using a single mode optical fibre interferometer', *Opt. Lett.*, 1980, **5**, p. 139
2 BUCARO, J. A., DARDY, H. D., and CARDME, J.: 'Fibre-optic hydrophone', *J. Acoust. Soc. Am.*, 1977, **62**, pp. 1302
3 DANDRIDGE, A., TVETEN, A. B., SIGEL, G. H., WEST, E. J., and GIALLORENZI, T. G.: 'Optical fibre magnetic field sensors', *Electron. Lett.*, 1980, **16**, p. 408
4 TVETEN, A. B., DANDRIDGE, A., DAVIS, C. M., and GIALLORENZI, T. G.: 'Fibre-optic accelerometer', *ibid.*, 1980, **16**, p. 854
5 JACKSON, D. A., PRIEST, R., DANDRIDGE, A., and TVETEN, A. B.: 'Elimination of drift in a single mode optical fibre interferometer using a piezoelectrically stretched coiled fibre', *Appl. Opt.*, 1980, **19**, p. 2926

0013-5194/82/090392-02$1.50/0

PERFORMANCE OF FH-MFSK SERIAL SEARCH SYNCHRONISER FOR MOBILE RADIO

Indexing terms: Telecommunication, Synchronisation, Mobile radio systems

A scheme for coarse acquisition of an FH-MFSK spread-spectrum multiple-access system is proposed. Performance curves showing the behaviour of the scheme in terms of false alarm and miss rates are given for a simplified mobile radio transmission model (white Gaussian noise and Rayleigh distributed fading). An optimisation procedure to minimise the acquisition mean time is outlined.

Introduction: To provide digital mobile radio telephony communication services to a great number of users, spread-spectrum modulation techniques using FH-MFSK (frequency hopped-multiple frequency shift keying) have been investigated recently with promising results.[1]

By assigning a distinct L tone sequence, called an adress, to each user, FH-MFSK allows many users (M) to share the same frequency band. In this multiple-access modulation scheme, each user transmits his information in blocks of K bits. Then, every T s L tones (chosen from a 2^K frequency alphabet) are transmitted. Details of the above modulation are given in Reference 1.

The transmitted messages can only be recovered if transmitter and receiver tone sequence generators are properly synchronised. The synchronisation process can be divided into the acquisition and the tracking phase. In this letter a serial search synchroniser to accomplish the initial acquisition phase of FH-MFSK sequences is proposed and its performance calculated.

Transmission model: If we assume that the address code for each mobile is randomly generated, the probability of N users transmitting the same chip frequency ω_l ($l = 1, 2, \ldots, L$) in any chip interval of duration $\tau = T/L$ s is

$$P_N = \binom{M}{N}\left(\frac{1}{2^K}\right)^N\left(1-\frac{1}{2^K}\right)^{M-N}$$

If $M \gg 1$ and $2^K \gg 1$, we can approximate the above binomial distribution by a Poisson distribution, obtaining

$$P_N \simeq \frac{(\lambda\tau)^N}{N!}\exp(-\lambda\tau) \quad \text{and} \quad \lambda = \frac{M}{\tau 2^K}$$

The Poisson approach makes it feasible to calculate the effect of the presence of mobile nonsynchronous users.

The receiver multiuser signal in the base station corresponding to the above generic chip frequency ω_l is

$$z(t) = \mathrm{Re}\{\underbrace{[R\exp(-j\theta)\,\mathrm{rect}_\tau(t-l\tau-\Delta t)}_{a} + \underbrace{\sum_{i=-\infty}^{\infty} R_i\exp(-j\theta_i)\,\mathrm{rect}_\tau(t-t_i)+n(t)}_{b}]\exp(-j\omega_l t)\} \quad (1)$$

where a corresponds to the desired signal, b corresponds to the multiuser interference signal, R, $\{R_i\}$ are independent Rayleigh random variables, θ, $\{\theta_i\}$ are independent $[0, 2\pi]$ uniform random variables, independent of the R, $\{R_i\}$,

$$\mathrm{rect}_\tau(t) = \begin{cases}1 & 0 \le t < \tau\\ 0 & \text{otherwise}\end{cases}$$

Δt is a parameter to be estimated with the serial search acquisition method, $n(t)$ is a white Gaussian noise $[n(t) = n_x(t) + jn_y(t)]$ of zero mean and $E(n_x^2) = E(n_y^2) = \sigma_n^2$.

Synchroniser description: The functional diagram of the acquisition system proposed to estimate Δt is shown in Fig. 1. When one user wants to initiate a transmission, he sends repeatedly the code adress of the called user as sync preample, i.e. $\omega_1, \omega_2, \ldots, \omega_L, \omega_1, \omega_2, \ldots, \omega_L, \omega_1, \ldots$. The L successive tones are tuned by L receiver filters and detected by an envelope detector followed by a threshold decision circuit (c_0 is the threshold value). The commutator C sweeps the L positions sequentially every T s. When the commutator C stops in a filter position coinciding with the arrival of the chip tone tuned to it, synchronisation is reached and the search control should stop after D successive positive tests. Otherwise the position of the reference sequence is changed by one increment, $\Delta\tau = \tau/n$, and the process will go on until D successive positive tests enter the search control.

Synchroniser performance: The presence of multiuser interference and noise degrades the performance of the synchroniser. The false alarm rate F_1 and the miss rate M_1 for one test are in this case:

$$F_1 = \sum_{i=L_{TH}}^{L}\binom{L}{i}P_{fa}^i(1-P_{fa})^{L-i}$$

$$M_1 = \sum_{i=0}^{L_{TH}-1}\binom{L}{i}(1-P_{miss})^i P_{miss}^{L-i}$$

P_{fa} is the probability of detecting energy when no desired tone was sent and P_{miss} is the probability of missing the tone sent. Both values can be calculated[2] from eqn. 1 as:

$$P_{fa} = \exp\left(-\frac{\beta^2}{2}\right)\exp(-\lambda\tau) + \sum_{m=1}^{\infty}\exp\left(-\frac{\beta^2}{2m\rho}\right)\exp(-\lambda\tau)\frac{(\lambda\tau)^m}{m!}$$

$$P_{miss} = \sum_{m=1}^{\infty}\left\{1-\exp\left[-\frac{\beta^2}{2(1+m\rho)}\right]\right\} \times \exp(-\lambda\tau)\frac{(\lambda\tau)^{m-1}}{(m-1)!}$$

where

$$\beta = \frac{c_0}{\sigma_n} \quad \text{and} \quad \rho = \frac{E(R^2)}{2\sigma_n^2}$$

After D successive tests, the false alarm rate F_D and the miss rate M_D are:

$$F_D = F_1^D$$

$$M_D = 1-\left[1-\sum_{i=0}^{L_{TH}-1}\binom{L}{i}(1-P_{miss})^i P_{miss}^{L-i}\right]^D \simeq DM_1$$

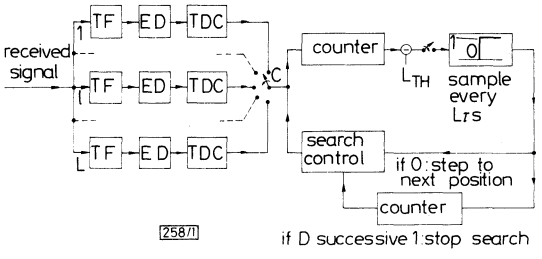

Fig. 1 *Functional diagram of FH-MFSK synchroniser*
TF = tuned filter
ED = envelope detector
TDC = threshold decision circuit

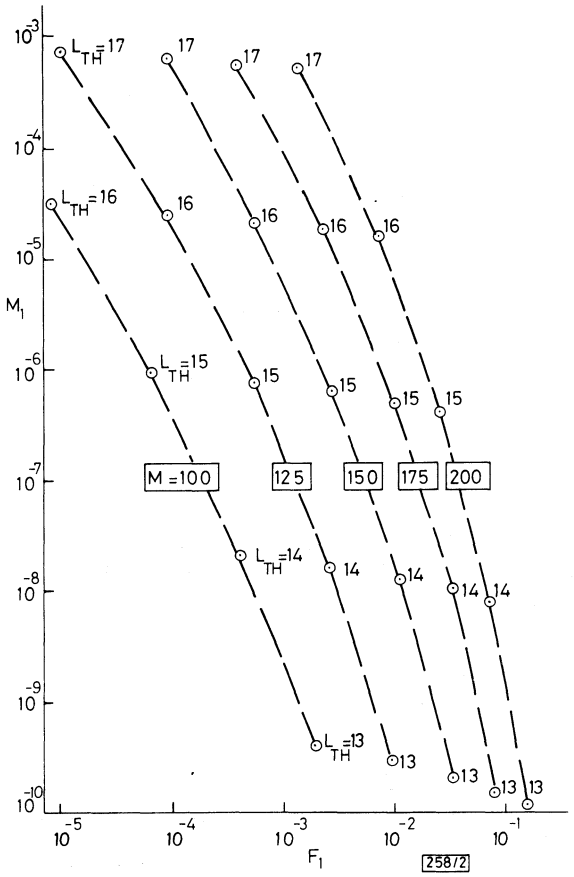

Fig. 2 *False alarm and miss error rates*
$\beta = 2{\cdot}75$
$\rho = 25$ dB

For a final desired value of F_D, an optimisation procedure can be envisaged to calculate the L_{TH} and D optimum values that minimise the acquisition mean time given by

$$E(t_{aq}) = DT + \frac{1 + nL}{2} S\tau \qquad (2)$$

where S represents the average number of chip intervals between two shifts of the reference signal. The value of S is calculated by

$$S = L + LF_1 + LF_1^2 + \ldots + LF_1^D = L\frac{1 - F_1^{D+1}}{1 - F_1}$$

$$\simeq \frac{L}{1 - F_1}$$

In Fig. 2 M_1 and F_1 are plotted for different M and L_{TH} values. We have considered a typical $\rho = 25$ dB and $L = 19$, $K = 8$ and $\beta = 2{\cdot}75$ (see Reference 1).

Regarding Fig. 2, and considering $E(t_{aq})$ given by eqn. 2, we can quickly obtain by trial and error the L_{TH} and D optimum values for a final F_D and M_D rates. For example, for $F_D < 10^{-4}$, $M_D < 10^{-4}$ and $M \leq 200$, the optimum design values are $D = 2$ and $L_{TH} = 16$ because for $L_{TH} = 17$ is $F_D > 10^{-4}$ and for $L_{TH} = 15$, $D = 3$ is needed and $E(t_{aq})$ is not minimum.

R. AGUSTI-COMES
G. JUNYENT-GIRALT
ETSI Telecomunicación
Apdo. 30.002, Barcelona, Spain

22nd February 1982

References

1 GOODMAN, D. J., HENRY, P. S., and PRABHU, V. K.: 'Frequency-hopped multilevel FSK for mobile radio', *Bell Syst. Tech. J.*, 1980, **59**, pp. 1257–1275
2 SCHWARTZ, M., BENNET, W. R., and STEIN, S.: 'Communication systems and techniques' (McGraw-Hill, 1966)

0013-5194/82/090393-03$1.50/0

COMMENT

FUNDAMENTAL MODE SPOT-SIZE MEASUREMENT IN SINGLE-MODE OPTICAL FIBRES

The author read with great interest the recent publication by Alard *et al.*[1] on equivalent step index (ESI) characterisation for monomode optical fibres, derived by an alternative measurement technique to that in their Reference 4.[2] In response to criticisms of the work in their Reference 4, the author would like to report the following points which are supported by recent experiments.

It is stated that the launch optics used in Reference 4 are incompatible with accurate loss measurements. This is not the case because the equipment is the same as a standard spectral loss measurement system. The only additional equipment to the spectral loss gear in the offset splice method of equivalent step index (ESI) determination[2] is one calibrated micropositioning slide. The axial separation and lateral offset directions are not critical parameters in the experiment. Furthermore, a completely automated measurement system using proprietary spectral loss equipment is soon to be reported.[3]

There is an indication in the work of Alard *et al.* that additional fibre handling may be a practical difficulty. It is agreed that the operator must first break and recleave the piece of fibre under test, but the cleaving tools and end-evaluation machines[4] are now available to do this job quickly and easily. It is noted that a properly cleaved end face would also be required for the variable-aperture excitation technique.

Loss measurements per unit length are difficult and inaccurate with short lengths of fibre. However the ESI technique[2] is not measuring spectral loss but the spectral variation of the fibre mode field width. The ESI measurement can only be carried out using a short length of fibre because the refractive-index profile (and hence the LP_{11} mode cutoff) varies with distance along it. The ESI measurement is a single-point measurement, that point in the fibre being at the moveable joint. The 'cut-back' short-length fibre universally used in spectral loss measurements is ideal for routine ESI characterisation using the same apparatus.

The technique in the original work[2] is not very dependent on the length of the short piece of fibre before or after the joint or on the presence of bends or microbends in the fibre. The measurement is of mode field-width not mode power content. The power is normalised at each wavelength because the e^{-1} field width is the displacement where the transmitted power falls to e^{-1} of its maximum value at that wavelength.

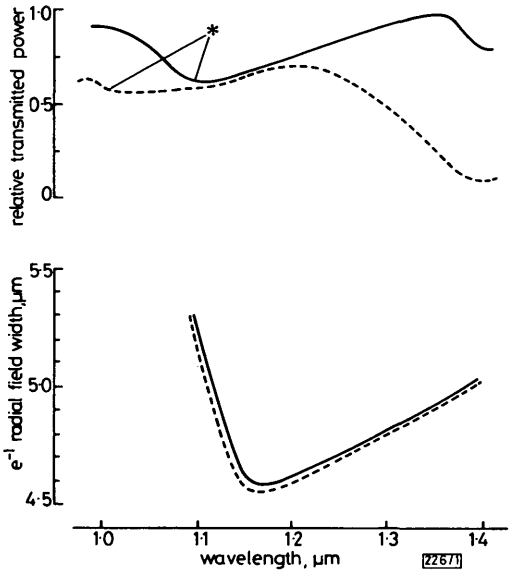

Fig. 1 *Effect of fibre bend on cutoff wavelength by transmitted power dips and by field-width measurement*
Fibre WASA 41
——— no small-radius bends
– – – – semicircular 6·5 mm bend in donor fibre between launch and first cladding mode stripper
* estimates of cutoff wavelengths from transmitted power dips

The position of the mode cutoff by this ESI method is not very dependent on the relative mode powers in the $LP_{01} + LP_{11}$ mode combination, whereas the estimation of cutoff by transmitted power reduction is prone to shifting due to length- and mode-dependent attenuation. Consider the example shown in Fig. 1. The ESI plot of field-width against wavelength is not altered by a semicircular 6·5 mm bend before the first cladding mode stripper (equivalent to a 2·4 dB power reduction at 1·3 μm wavelength). On the other hand, the maximum power transmitted through the system gives an apparent shift in the cutoff wavelength as estimated by a dip in the transmitted power. In Fig. 2, the length of fibre up to the joint was shortened from 1000 mm to 320 mm. The transmitted power dip leads to an ambiguous cutoff, but the field-width plot remains largely unchanged.

It is accepted that the LP_{11} mode cutoff position determined by the crossover of the extrapolations to the sections of the field-width plot of Fig. 2 of Reference 2 is a defined point, and has yet to be rigorously proven. However, results indicate that it is a sensible choice because the spot-size variation with wavelength is correct to within the experimental measurement accuracy, and comparisons with refracted near-field refractive-index profiles are good. The use of ESI data gives excellent agreement with cascaded fibre system performance. The method of fitting straight lines to the measured data points, which was used in our original work, is more prone to error than more elaborate curve-fitting techniques